Electronic Supplementary Information for

Sialylation-Induced Stabilization of Dynamic Glycoprotein Conformations Unveiled by Time-Aligned Parallel Unfolding and Glycan Releasing Mass Spectrometry

Yifei Jia,[a‡] Yichang Liu,[b‡] Yamei Wang,[a‡] Jinyu Li,[d,] and Gongyu Li, [a,c,*]*

[a]Tianjin Key Laboratory of Biosensing and Molecular Recognition, Research Center for Analytical Science, Frontiers Science Center for New Organic Matter, College of Chemistry, Nankai University, Tianjin 300071, China.

[b]School of Pharmacy, Nantong University, Nantong 226001, Jiangsu, China.

[c]Haihe Laboratory of Sustainable Chemical Transformations, Tianjin 300192, China.

[d]College of Chemistry, Fuzhou University, Fuzhou 350108, Fujian, China.

‡ Y.J., Y.L. and Y.W. contributed equally to this work.

* Corresponding author:

Prof. Dr. Gongyu Li, Email: ligongyu@nankai.edu.cn

Prof. Dr. Jinyu Li, Email: j.li@fzu.edu.cn

Table of Contents:

Supplementary Experimental

Glycoproteomic sample preparation. Glycoproteins were first denatured by heating at 95 ℃ for 5 min. The samples were then treated with 10 mM DTT by incubation at 37 ℃ for 30 min to reduce the disulfide bonds. After reduction, the samples were alkylated with 50 mM IAA for 30 min in the dark to block the reduced cysteine. The samples were quenched by adding 10 mM DTT for 5 min. 50 mM Tris-HCl (pH 8.0) and trypsin (protein: trypsin, 50:1, w/w) were added to the samples and incubated at 37 ℃ overnight. Digestion was terminated by adding trifluoroacetic acid (TFA) to a final concentration of 0.25%, and particulate material was removed by centrifugation at 14,000 g for 20 min. Sample mixture was desalted using a SepPak C18 SPE cartridge (Waters, Milford, MA).

LC-MS/MS analysis. Samples were analyzed on an Orbitrap Fusion Lumos Tribrid mass spectrometer coupled to a Dionex UltiMate 3000 UPLC (Thermo Fisher Scientific). A binary solvent system composed of H_2O containing 0.1% FA (A) and ACN containing 0.1% FA (B) was used for all analyses. Samples were loaded and separated on an in-house made 15 cm capillary (75 μm i.d.) packed using 1.7 μm diameter Ethylene Bridged Hybrid (BEH) C18 material obtained from a Waters UPLC column. The LC gradient for N-glycopeptides was set as follows, 3%–30% A (18–73 min), 75% A (73–83 min), and 95% A (83–93 min), 3% A (93–108 min). The mass spectrometer was operated in data-dependent acquisition mode to automatically switch between MS and MS/MS acquisition. For intact N-glycopeptides analysis, an MS1 scan (*m/z*) was acquired from 375 to 2000 (120,000 resolution, 2.0e5 AGC, injection time 50 ms) followed by HCD MS/MS acquisition of the precursors with fixed HCD collision energy (%) 30, and detected in the Orbitrap (30,000 resolution, 5.0e4 AGC, maximum injection time 54 ms). EThcD was triggered by HCD fragment *m/z* 204.0867, *m/z* 138.0545, *m/z* 366.1396 with a mass tolerance of 15 ppm. The scan range (*m/z*) was 150-2000 (30,000 resolution, 5.0e4 AGC, maximum injection time 54 ms).

Glycoproteomics data analysis. Raw data files were searched using Byonic (Protein Metrics Inc., San Carlos, CA) embedded within Proteome Discoverer 2.5 (Thermo Fisher Scientific)

against the UniProt database (including UniProt ID: P12763, P02765, Q58D62, Q9UGM5). Trypsin was selected as the enzyme and two maximum missed cleavages were allowed. Searches were performed with a precursor mass tolerance of 15 ppm and a fragment mass tolerance of 0.01 Da. Static modifications consisted of carbamidomethylation of cysteine residues (+ 57.02146 Da). Dynamic modifications consisted of oxidation of methionine residues (+ 15.99492 Da), deamidation of asparagine and glutamine (+ 0.98402 Da), and N-glycosylation on asparagine. Oxidation and deamidation were set as "rare" modification, and N-glycosylation was set as "common" modification through Byonic node. Mammalian N-glycan database embedded in Byonic, which contains 309 glycan entities, was used. Results were filtered to a 1% protein FDR as set in the Byonic parameters, and data was further processed to 1% FDR at the PSM level using the 2D-FDR score. Further filters added were unambiguous PSM and protein assignment, Byonic score cut-off >100, |Log Prob|> 1, and delta mod score > 10. For the glycan-protein network, N-glycopeptides were exclusively categorized into six glycan type categories based on glycan composition: (1) Sialylated and fucosylated (2) sialylated (containing sialic acid) only; (3) fucosylated (containing fucose) only; (4) complex/hybrid (> 2 HexNAc); (5) high mannose (2 HexNAc and ≥ 5 Hex), and (6) paucimannose (2 HexNAc and < 5 Hex).

Molecular dynamics (MD) simulations

The starting 3D structure of the bFT (AlphaFoldDB: P12763) was obtained from the AlphaFold database.[1] The glycoform on Asn99 and Asn156 in bFT was randomly selected based on our glycoproteomic results (Table S2). To our knowledge, at present, there is no commercially available enzyme for this linkage-specific removal of sialic acids. The widely used sialidase was unable to distinct between α2,3- and α2,6-linked sialic acids. In our study, we found that the di-sialylated glycoform predominated in bFT, while the mono-sialylated form was most abundant in hFT. Notably, it has been reported that although both α-2,3 and α-2,6 linkage isoforms of sialic acid exist in bFT,[2] di-sialylated form bFT and the mono-sialylated form hFT mainly carry the α2,6-linked sialic acid. Therefore, α-2,6-linked sialic acid was chosen for the MD simulations as a proof-of-concept demonstration. The geometries and the partial charge of the glycosyl carboxamide as well as the modified asparagine residues were optimized by

Gaussian 09 package at the B3LYP/6-31G* level of theory.[3, 4] The classical three-point rigid water model TIP3P were used for the solvent.[5] The Amber14SB force field was used for proteins and ions.[6] The protein was placed in the center of the box with a size of $130 \times 130 \times 130$ Å^3 and the concentration of NaCl was 0.15 M. The periodic boundary conditions were employed on all three dimensions.

All MD simulations were performed in Amber20 software with the in-house GPU clusters acceleration.[7] A 10 Å cut-off value was used for treating the noncovalent interactions. The particle mesh Ewald (PME) algorithm was applied for calculating the electrostatic interactions.[8] All bonds involving hydrogen were constrained using the SHAKE algorithm.[9] The time step was set to 2 fs in this work. Before the productive MD simulation, energy minimization (5000 steps steepest descent algorithm was followed by 5000 steps conjugated gradient method) was performed to make sure the system has no inappropriate geometry or steric clashes.[10] The minimized simulation cell was heated and maintained at 300 K for 0.5 ns using the Langevin dynamics algorithm.[11, 12] Then, the system was equilibrium for 5 ns to achieve constant pressure (1 bar) in the isothermal-isobaric (NPT) ensemble in control of the Berendsen barostat.[13] Finally, 1000 ns classical MD simulation was carried out for data collection.

To investigate the unfolding pathways of bFT and asialofetuin (Asialo), the heating MD simulations in both aqueous solution and gas phase were performed. The 500 ns production simulations were run over a linear temperature gradient of 300-750 K. For the gas-phase MD simulations, the protonation state of each system was predicted with a well-established hybrid Monte Carlo/molecular dynamics (MC/MD) protocol developed by us previously.[14-16] The default setup and parameters were applied in this work.

For each system investigated in this work, three parallel simulations were performed with different velocity generation seeds to estimate the statistical uncertainties. The equilibrium MD trajectory of each simulation was used for analysis. Cluster analysis was applied using the density-based spatial clustering of applications with noise (DBSCAN) algorithm to identify the most representative structures. The hydrogen bonds (X-H…X; X=F, N, and O) were defined

as follows: (a) $d_{xx} \leq 3.5$ Å; (b) $\theta_{xx} \geq 150^{\circ}$.[17, 18] The contact numbers were defined as the number of atom-pairs with atomic distances smaller than 6 Å. The melting temperature, Tm, was defined as the temperature at which the averaged secondary structural content decreased to 50%.

2-NBDG Uptake. 2-NBDG (2-(*N*-(7-Nitrobenz-2-oxa-1,3-diazol-4-yl)Amino)-2-Deoxyglucose, ThermoFisher, N13195) is a fluorescently labeled 2-deoxyglucose analogue that competitively inhibits with D-glucose and can therefore be used as a tracer for glucose metabolism in cells (Amgicam, AJCI4820). The HepG2 cells ($1.5x10^4$ cells/wall) were cultured in 96-well plates overnight, washed with PBS, and incubated with 200 μg/mL sialo- and/or asialo-FAB at 37°C for 4 hours, then washed with PBS for 3 times. Adding 100 nM insulin and incubation for 30 min, followed by addition of 100 μM 2-NBDG and incubation for 15 min. The cells were washed with PBS and the fluorescence intensity was measured with 485 nm excitation and 520 nm emmision. All experiments were performed at least with six biological replicates.

Supplementary Figures

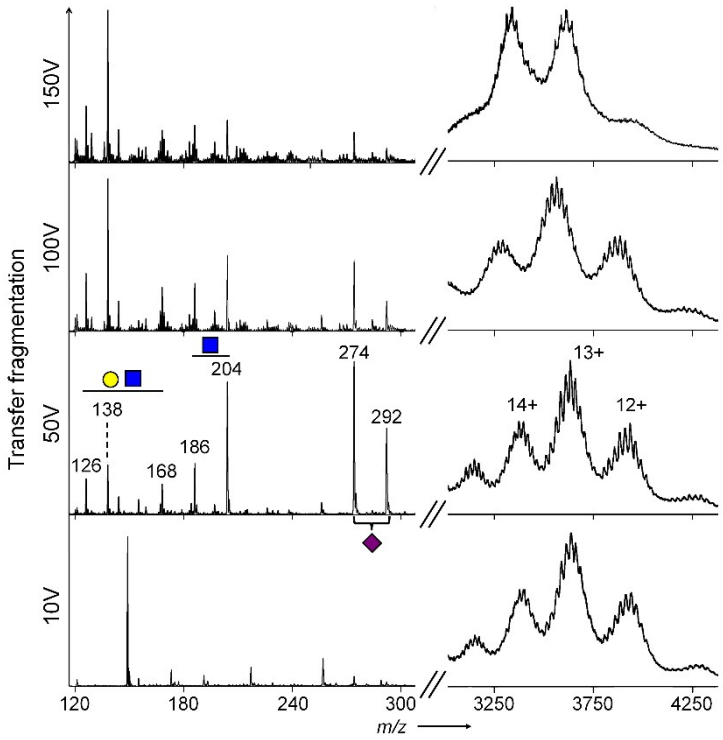

Figure S1. Representative native MS data for bFT with trap CE at 10 V and transfer fragmentation at 10 V to 150 V.

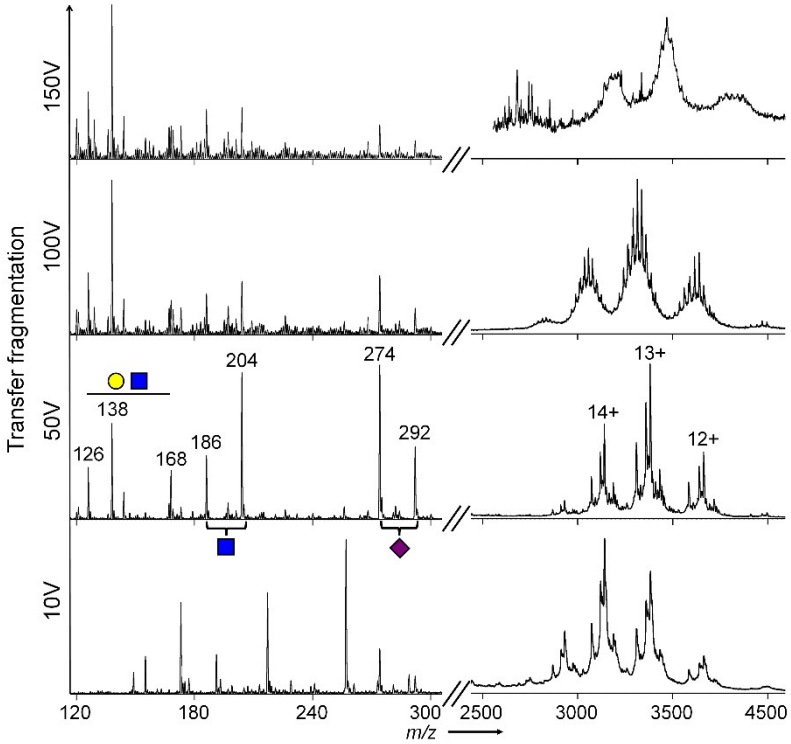

Figure S2. Representative native MS data for hFT with trap CE at 10 V and transfer fragmentation at 10 V to 150 V.

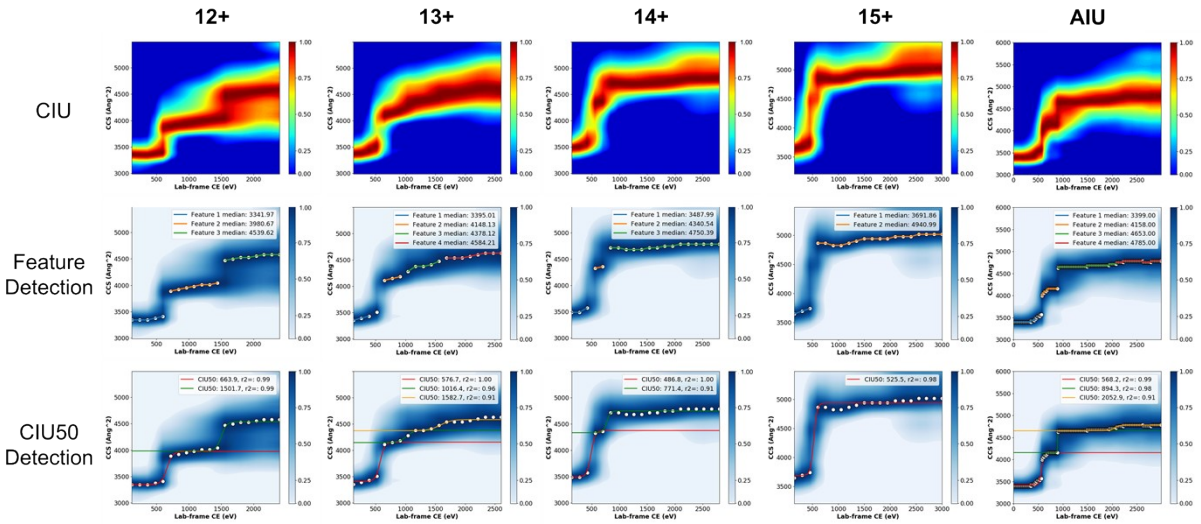

Figure S3. Charge-separated and all-ion unfolding fingerprints for bFT.

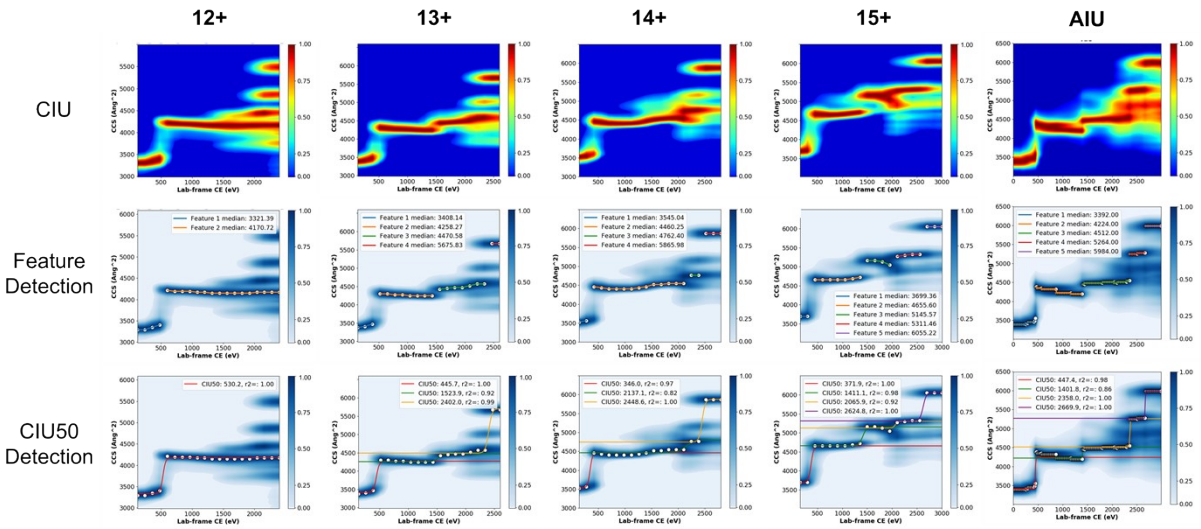

Figure S4. Charge-separated and all-ion unfolding fingerprints for hFT.

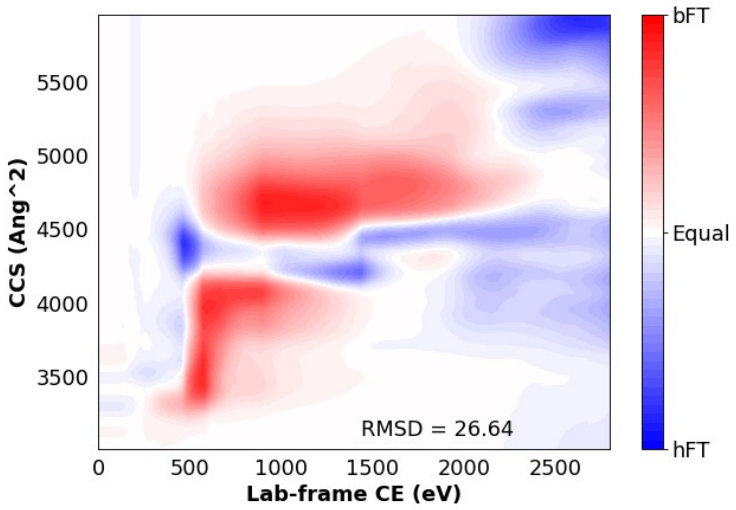

Figure S5. AIU RMSD distribution of bFT compared with hFT.

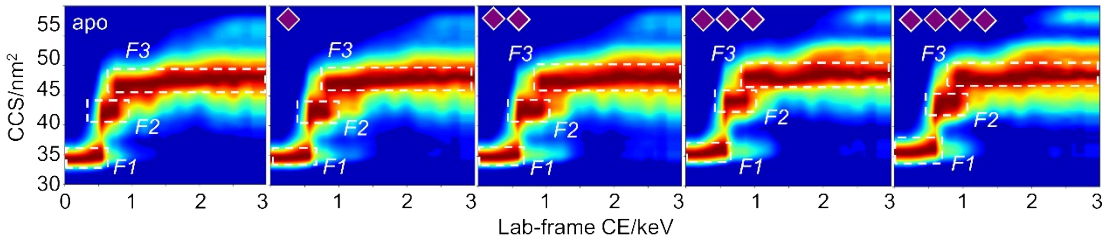

Figure S6. Representative AIU fingerprints of bFT with different sialoforms.

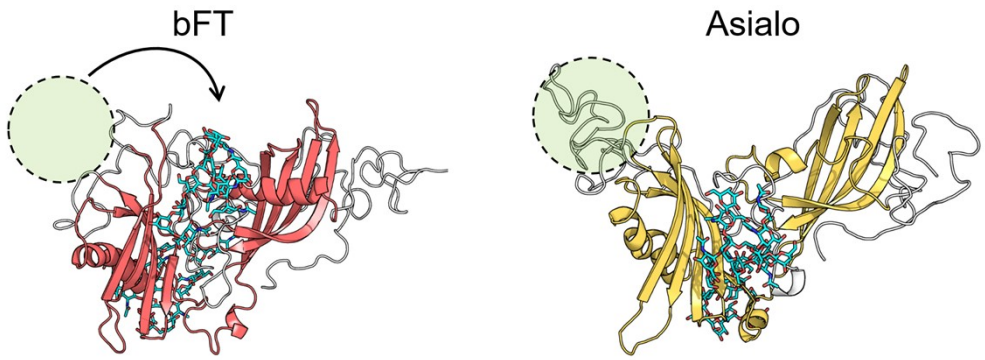

Figure S7. The representative structures of bFT and Asialo in aqueous solution. The loop 255-298 was highlighted in light green circles. The modification groups were represented by sticks (carbon: cyan, nitrogen: blue, oxygen: red).

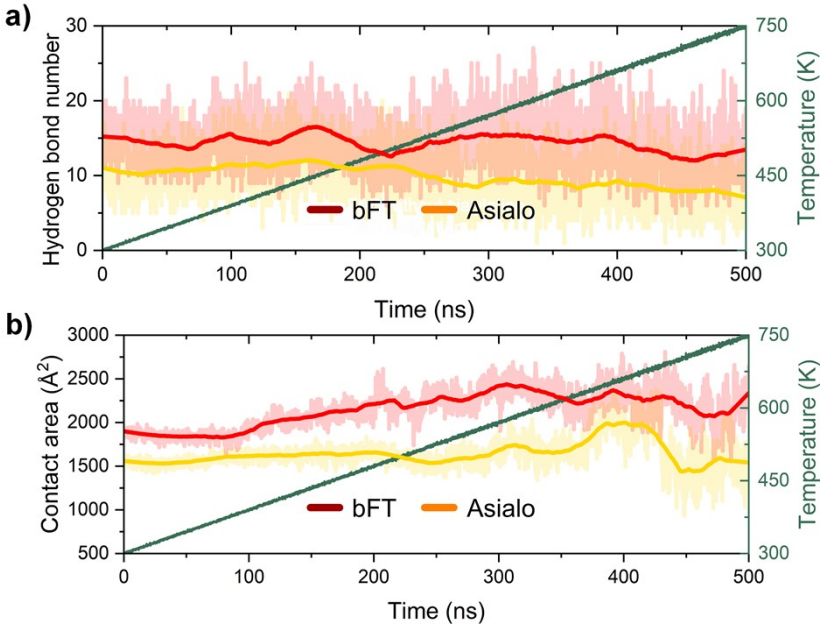

Figure S8. Hydrogen bond number (a) and contact area (b) between glycans and bFT or asialo-bFT during aqueous-solution heating MD simulations.

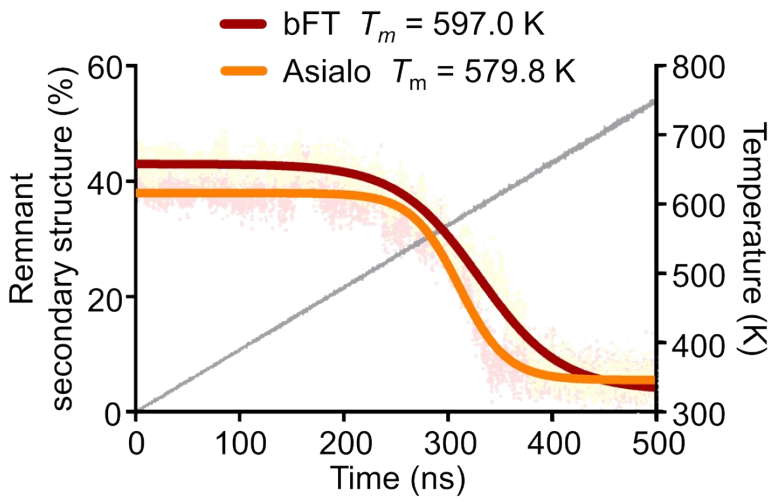

Figure S9. Percentage of remnant secondary structure of bFT and asialo-bFT during aqueous-solution heating MD simulations.

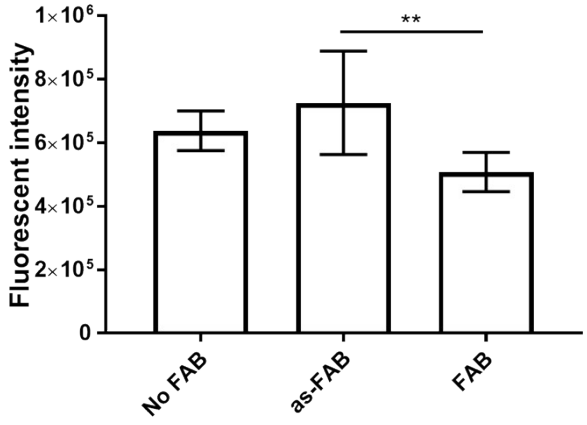

Figure S10. Effect of fetuin sialylation in insulin-mediated glucose uptake. 2-NBDG, a fluorescent probe substrate, was selected for cellular glucose uptake monitoring. 200 μg/mL FAB or asialo-FAB (as-FAB) were used. Data were expressed as mean ± SD (n=6). Inter-group comparisons were analyzed using one-way ANOVA analysis (**p <0.01).

Supplementary Tables

Table S1. Comparison of secondary structure contents for bFT and hFT based on their 3D structures.

	bFT	hFT
α-helix	21.73%	22.07%
β-sheet	18.11%	18.53%
β-turn	3.06%	3.27%
Random coil	57.10%	56.13%
Sequence identity	65.07%	

Table S2. Information for bFT N-glycosylation identified from glycoproteomic experiments.

Annotated Sequence	Accession	Sites	Glycan Composition
[R].KLCPDCPLLAPLNDSR.[V]	P12763	P12763 [144-159]	HexNAc(4)Hex(5)
[R].KLCPDCPLLAPLNDSR.[V]	P12763	P12763 [144-159]	HexNAc(4)Hex(5)NeuAc(1)
[R].KLCPDCPLLAPLNDSR.[V]	P12763	P12763 [144-159]	HexNAc(5)Hex(6)
[R].KLCPDCPLLAPLNDSR.[V]	P12763	P12763 [144-159]	HexNAc(4)Hex(5)NeuAc(2)
[R].KLCPDCPLLAPLNDSR.[V]	P12763	P12763 [144-159]	HexNAc(5)Hex(6)NeuAc(1)
[R].KLCPDCPLLAPLNDSR.[V]	P12763	P12763 [144-159]	HexNAc(6)Hex(6)Fuc(2)
[R].KLCPDCPLLAPLNDSR.[V]	P12763	P12763 [144-159]	HexNAc(5)Hex(6)NeuAc(2)
[R].KLCPDCPLLAPLNDSR.[V]	P12763	P12763 [144-159]	HexNAc(5)Hex(6)NeuAc(3)
[K].LCPDCPLLAPLNDSR.[V]	P12763	P12763 [145-159]	HexNAc(1)
[K].LCPDCPLLAPLNDSR.[V]	P12763	P12763 [145-159]	HexNAc(2)
[K].LCPDCPLLAPLNDSR.[V]	P12763	P12763 [145-159]	HexNAc(3)Hex(4)
[K].LCPDCPLLAPLNDSR.[V]	P12763	P12763 [145-159]	HexNAc(4)Hex(4)
[K].LCPDCPLLAPLNDSR.[V]	P12763	P12763 [145-159]	HexNAc(4)Hex(5)
[K].LCPDCPLLAPLNDSR.[V]	P12763	P12763 [145-159]	HexNAc(5)Hex(5)
[K].LCPDCPLLAPLNDSR.[V]	P12763	P12763 [145-159]	HexNAc(4)Hex(5)NeuAc(1)
[K].LCPDCPLLAPLNDSR.[V]	P12763	P12763 [145-159]	HexNAc(4)Hex(5)Fuc(2)

[K].LCPDCPLLAPLNDSR.[V]	P12763	P12763 [145-159]	HexNAc(5)Hex(6)
[K].LCPDCPLLAPLNDSR.[V]	P12763	P12763 [145-159]	HexNAc(4)Hex(5)NeuAc(2)
[K].LCPDCPLLAPLNDSR.[V]	P12763	P12763 [145-159]	HexNAc(4)Hex(5)NeuAc(1)NeuGc(1)
[K].LCPDCPLLAPLNDSR.[V]	P12763	P12763 [145-159]	HexNAc(5)Hex(6)NeuAc(1)
[K].LCPDCPLLAPLNDSR.[V]	P12763	P12763 [145-159]	HexNAc(5)Hex(7)Fuc(1)
[K].LCPDCPLLAPLNDSR.[V]	P12763	P12763 [145-159]	HexNAc(5)Hex(6)NeuAc(2)
[K].LCPDCPLLAPLNDSR.[V]	P12763	P12763 [145-159]	HexNAc(5)Hex(6)Fuc(2)NeuAc(1)
[K].LCPDCPLLAPLNDSR.[V]	P12763	P12763 [145-159]	HexNAc(5)Hex(6)NeuAc(3)
[K].LCPDCPLLAPLNDSR.[V]	P12763	P12763 [145-159]	HexNAc(5)Hex(7)Fuc(1)NeuAc(2)
[R].VVHAVEVALATFNAESNGSYLQLVEISR.[A]	P12763	P12763 [160-187]	HexNAc(5)Hex(6)
[R].VVHAVEVALATFNAESNGSYLQLVEISR.[A]	P12763	P12763 [160-187]	HexNAc(5)Hex(6)
[R].VVHAVEVALATFNAESNGSYLQLVEISR.[A]	P12763	P12763 [160-187]	HexNAc(5)Hex(6)NeuAc(1)
[R].VVHAVEVALATFNAESNGSYLQLVEISR.[A]	P12763	P12763 [160-187]	HexNAc(5)Hex(6)NeuAc(1)
[R].VVHAVEVALATFNAESNGSYLQLVEISR.[A]	P12763	P12763 [160-187]	HexNAc(5)Hex(6)NeuAc(3)
[R].VVHAVEVALATFNAESNGSYLQLVEISR.[A]	P12763	P12763 [160-187]	HexNAc(5)Hex(6)NeuAc(3)
[R].VVHAVEVALATFNAESNGSYLQLVEISR.[A]	P12763	P12763 [160-187]	HexNAc(5)Hex(6)Fuc(1)NeuAc(2)NeuGc(1)
[R].VVHAVEVALATFNAESNGSYLQLVEISR.[A]	P12763	P12763 [160-187]	HexNAc(6)Hex(7)NeuAc(4)
[R].RPTGEVYDIEIDTLETTCHVLDPTPLANCSVR.[Q]	P12763	P12763 [72-103]	HexNAc(4)Hex(5)

[R].RPTGEVYDIEIDTLETTCHVLDPTPLANCSVR.[Q]	P12763	P12763 [72-103]	HexNAc(4)Hex(5)NeuGc(1)
[R].RPTGEVYDIEIDTLETTCHVLDPTPLANCSVR.[Q]	P12763	P12763 [72-103]	HexNAc(4)Hex(6)Fuc(1)
[R].RPTGEVYDIEIDTLETTCHVLDPTPLANCSVR.[Q]	P12763	P12763 [72-103]	HexNAc(5)Hex(6)
[R].RPTGEVYDIEIDTLETTCHVLDPTPLANCSVR.[Q]	P12763	P12763 [72-103]	HexNAc(5)Hex(6)NeuAc(1)
[R].RPTGEVYDIEIDTLETTCHVLDPTPLANCSVR.[Q]	P12763	P12763 [72-103]	HexNAc(5)Hex(6)Fuc(2)

Table S3. Information for hFT N-glycosylation identified from glycoproteomic experiments.

Annotated Sequence	Accession	Sites	Glycan Composition
[K].AALAAFNAQNNGSNFQLEEISR.[A]	P02765	P02765 [166-187]	HexNAc(7)Hex(8)NeuGc(1)
[K].AALAAFNAQNNGSNFQLEEISR.[A]	P02765	P02765 [166-187]	HexNAc(7)Hex(8)Fuc(1)NeuAc(1)
[K].AALAAFNAQNNGSNFQLEEISR.[A]	P02765	P02765 [166-187]	HexNAc(6)Hex(7)Fuc(1)
[K].AALAAFNAQNNGSNFQLEEISR.[A]	P02765	P02765 [166-187]	HexNAc(5)Hex(7)Fuc(1)NeuAc(2)
[K].AALAAFNAQNNGSNFQLEEISR.[A]	P02765	P02765 [166-187]	HexNAc(5)Hex(7)Fuc(1)NeuAc(1)
[K].AALAAFNAQNNGSNFQLEEISR.[A]	P02765	P02765 [166-187]	HexNAc(5)Hex(6)NeuAc(3)
[K].AALAAFNAQNNGSNFQLEEISR.[A]	P02765	P02765 [166-187]	HexNAc(5)Hex(6)NeuAc(2)
[K].AALAAFNAQNNGSNFQLEEISR.[A]	P02765	P02765 [166-187]	HexNAc(5)Hex(6)Fuc(1)NeuAc(3)
[K].AALAAFNAQNNGSNFQLEEISR.[A]	P02765	P02765 [166-187]	HexNAc(5)Hex(6)Fuc(1)NeuAc(2)NeuGc(1)
[K].AALAAFNAQNNGSNFQLEEISR.[A]	P02765	P02765 [166-187]	HexNAc(5)Hex(3)Fuc(1)NeuAc(1)
[K].AALAAFNAQNNGSNFQLEEISR.[A]	P02765	P02765 [166-187]	HexNAc(4)Hex(7)Fuc(1)
[K].AALAAFNAQNNGSNFQLEEISR.[A]	P02765	P02765 [166-187]	HexNAc(4)Hex(6)NeuAc(1)
[K].AALAAFNAQNNGSNFQLEEISR.[A]	P02765	P02765 [166-187]	HexNAc(4)Hex(6)Fuc(1)NeuAc(1)
[K].AALAAFNAQNNGSNFQLEEISR.[A]	P02765	P02765 [166-187]	HexNAc(4)Hex(6)Fuc(1)
[K].AALAAFNAQNNGSNFQLEEISR.[A]	P02765	P02765 [166-187]	HexNAc(4)Hex(5)NeuAc(2)
[K].AALAAFNAQNNGSNFQLEEISR.[A]	P02765	P02765 [166-187]	HexNAc(4)Hex(5)NeuAc(1)

[K].AALAAFNAQNNGSNFQLEEISR.[A]	P02765	P02765 [166-187]	HexNAc(4)Hex(5)NeuAc(1)
[K].AALAAFNAQNNGSNFQLEEISR.[A]	P02765	P02765 [166-187]	HexNAc(4)Hex(5)Fuc(1)NeuAc(1)NeuGc(1)
[K].AALAAFNAQNNGSNFQLEEISR.[A]	P02765	P02765 [166-187]	HexNAc(4)Hex(5)Fuc(1)NeuAc(1)
[K].AALAAFNAQNNGSNFQLEEISR.[A]	P02765	P02765 [166-187]	HexNAc(4)Hex(5)NeuAc(2)
[K].AALAAFNAQNNGSNFQLEEISR.[A]	P02765	P02765 [166-187]	HexNAc(4)Hex(4)Fuc(2)
[K].AALAAFNAQNNGSNFQLEEISR.[A]	P02765	P02765 [166-187]	HexNAc(3)Hex(6)NeuAc(1)
[K].AALAAFNAQNNGSNFQLEEISR.[A]	P02765	P02765 [166-187]	HexNAc(4)Hex(5)Fuc(1)NeuAc(2)
[K].AALAAFNAQNNGSNFQLEEISR.[A]	P02765	P02765 [166-187]	HexNAc(3)Hex(4)NeuAc(1)
[K].AALAAFNAQNNGSNFQLEEISR.[A]	P02765	P02765 [166-187]	HexNAc(2)Hex(11)
[K].AALAAFNAQNNGSNFQLEEISR.[A]	P02765	P02765 [166-187]	HexNAc(1)Fuc(1)
[K].AALAAFNAQNNGSNFQLEEISR.[A]	P02765	P02765 [166-187]	HexNAc(1)
[K].AALAAFNAQNNGSNFQLEEISR.[A]	P02765	P02765 [166-187]	HexNAc(5)Hex(6)Fuc(1)NeuAc(2)
[K].AALAAFNAQNNGSNFQLEEISR.[A]	P02765	P02765 [166-187]	HexNAc(1)
[K].AALAAFNAQNNGSNFQLEEISR.[A]	P02765	P02765 [166-187]	HexNAc(5)Hex(6)NeuAc(3)
[K].AALAAFNAQNNGSNFQLEEISR.[A]	P02765	P02765 [166-187]	HexNAc(5)Hex(6)Fuc(1)NeuAc(3)
[K].AALAAFNAQNNGSNFQLEEISR.[A]	P02765	P02765 [166-187]	HexNAc(5)Hex(6)Fuc(1)NeuAc(2)
[K].AALAAFNAQNNGSNFQLEEISR.[A]	P02765	P02765 [166-187]	HexNAc(5)Hex(6)Fuc(3)NeuAc(1)
[K].AALAAFNAQNNGSNFQLEEISR.[A]	P02765	P02765 [166-187]	HexNAc(5)Hex(4)NeuAc(2)

[K].AALAAFNAQNNGSNFQLEEISR.[A]	P02765	P02765 [166-187]	HexNAc(4)Hex(7)
[K].CDSSPDSAEDVRKVCQDCPLLAPLNDTR.[V]	P02765	P02765 [132-159]	HexNAc(4)Hex(5)NeuAc(2)
[K].VCQDCPLLAPLNDTR.[V]	P02765	P02765 [145-159]	HexNAc(5)Hex(7)Fuc(1)NeuAc(2)
[K].VCQDCPLLAPLNDTR.[V]	P02765	P02765 [145-159]	HexNAc(5)Hex(6)NeuAc(3)
[K].VCQDCPLLAPLNDTR.[V]	P02765	P02765 [145-159]	HexNAc(5)Hex(6)NeuAc(2)
[K].VCQDCPLLAPLNDTR.[V]	P02765	P02765 [145-159]	HexNAc(5)Hex(6)NeuAc(1)
[K].VCQDCPLLAPLNDTR.[V]	P02765	P02765 [145-159]	HexNAc(5)Hex(6)Fuc(1)NeuAc(3)
[K].VCQDCPLLAPLNDTR.[V]	P02765	P02765 [145-159]	HexNAc(5)Hex(6)Fuc(1)NeuAc(1)NeuGc(1)
[K].VCQDCPLLAPLNDTR.[V]	P02765	P02765 [145-159]	HexNAc(4)Hex(7)NeuAc(1)
[K].VCQDCPLLAPLNDTR.[V]	P02765	P02765 [145-159]	HexNAc(4)Hex(6)NeuAc(1)
[K].VCQDCPLLAPLNDTR.[V]	P02765	P02765 [145-159]	HexNAc(4)Hex(6)Fuc(1)
[K].VCQDCPLLAPLNDTR.[V]	P02765	P02765 [145-159]	HexNAc(4)Hex(5)NeuAc(2)
[K].VCQDCPLLAPLNDTR.[V]	P02765	P02765 [145-159]	HexNAc(5)Hex(6)Fuc(1)NeuAc(2)
[K].VCQDCPLLAPLNDTR.[V]	P02765	P02765 [145-159]	HexNAc(4)Hex(5)Fuc(1)NeuAc(2)
[K].VCQDCPLLAPLNDTR.[V]	P02765	P02765 [145-159]	HexNAc(4)Hex(5)NeuAc(1)NeuGc(1)
[K].VCQDCPLLAPLNDTR.[V]	P02765	P02765 [145-159]	HexNAc(4)Hex(5)NeuAc(1)
[K].VCQDCPLLAPLNDTR.[V]	P02765	P02765 [145-159]	HexNAc(4)Hex(5)Fuc(2)NeuAc(1)
[K].VCQDCPLLAPLNDTR.[V]	P02765	P02765 [145-159]	HexNAc(4)Hex(5)Fuc(2)

[K].VCQDCPLLAPLNDTR.[V]	P02765	P02765 [145-159]	HexNAc(4)Hex(5)Fuc(1)NeuAc(1)
[K].VCQDCPLLAPLNDTR.[V]	P02765	P02765 [145-159]	HexNAc(4)Hex(5)
[K].VCQDCPLLAPLNDTR.[V]	P02765	P02765 [145-159]	HexNAc(4)Hex(4)NeuAc(1)
[K].VCQDCPLLAPLNDTR.[V]	P02765	P02765 [145-159]	HexNAc(3)Hex(4)NeuAc(1)
[K].VCQDCPLLAPLNDTR.[V]	P02765	P02765 [145-159]	HexNAc(2)Hex(8)
[K].VCQDCPLLAPLNDTR.[V]	P02765	P02765 [145-159]	HexNAc(1)
[K].VCQDCPLLAPLNDTRVVHAAK.[A]	P02765	P02765 [145-165]	HexNAc(4)Hex(5)NeuAc(2)
[R].KVCQDCPLLAPLNDTR.[V]	P02765	P02765 [144-159]	HexNAc(7)Hex(8)NeuAc(1)
[R].KVCQDCPLLAPLNDTR.[V]	P02765	P02765 [144-159]	HexNAc(5)Hex(6)NeuAc(3)
[R].KVCQDCPLLAPLNDTR.[V]	P02765	P02765 [144-159]	HexNAc(5)Hex(6)NeuAc(2)
[R].KVCQDCPLLAPLNDTR.[V]	P02765	P02765 [144-159]	HexNAc(5)Hex(6)Fuc(1)NeuAc(3)
[R].KVCQDCPLLAPLNDTR.[V]	P02765	P02765 [144-159]	HexNAc(4)Hex(6)NeuAc(1)
[R].KVCQDCPLLAPLNDTR.[V]	P02765	P02765 [144-159]	HexNAc(4)Hex(5)NeuAc(2)
[R].KVCQDCPLLAPLNDTR.[V]	P02765	P02765 [144-159]	HexNAc(4)Hex(5)NeuAc(1)
[R].KVCQDCPLLAPLNDTR.[V]	P02765	P02765 [144-159]	HexNAc(4)Hex(5)Fuc(3)
[R].KVCQDCPLLAPLNDTR.[V]	P02765	P02765 [144-159]	HexNAc(4)Hex(5)Fuc(1)NeuAc(2)
[R].KVCQDCPLLAPLNDTR.[V]	P02765	P02765 [144-159]	HexNAc(4)Hex(5)Fuc(1)NeuAc(1)
[R].KVCQDCPLLAPLNDTR.[V]	P02765	P02765 [144-159]	HexNAc(3)Hex(4)NeuAc(1)

[R].KVCQDCPLLAPLNDTR.[V]	P02765	P02765 [144-159]	HexNAc(5)Hex(6)Fuc(1)NeuAc(2)

Table S4. Information for asialo-bFT N-glycosylation identified from glycoproteomic experiments.

Annotated Sequence	Accession	Sites	Glycan Composition
[R].KLCPDCPLLAPLNDSR.[V]	P12763	P12763 [144-159]	Hex(3)HexNAc(3)
[R].KLCPDCPLLAPLNDSR.[V]	P12763	P12763 [144-159]	Hex(5)HexNAc(4)
[R].KLCPDCPLLAPLNDSR.[V]	P12763	P12763 [144-159]	Hex(4)HexNAc(3)
[R].KLCPDCPLLAPLNDSR.[V]	P12763	P12763 [144-159]	Hex(5)HexNAc(4)
[R].KLCPDCPLLAPLNDSR.[V]	P12763	P12763 [144-159]	Hex(5)HexNAc(4)
[R].KLCPDCPLLAPLNDSR.[V]	P12763	P12763 [144-159]	Hex(6)HexNAc(5)Fuc(2)
[K].LCPDCPLLAPLNDSR.[V]	P12763	P12763 [145-159]	Hex(6)HexNAc(5)
[K].LCPDCPLLAPLNDSR.[V]	P12763	P12763 [145-159]	Hex(6)HexNAc(5)
[K].LCPDCPLLAPLNDSR.[V]	P12763	P12763 [145-159]	Hex(5)HexNAc(4)
[K].LCPDCPLLAPLNDSR.[V]	P12763	P12763 [145-159]	Hex(3)HexNAc(3)
[K].LCPDCPLLAPLNDSR.[V]	P12763	P12763 [145-159]	Hex(9)HexNAc(2)Fuc(1)
[K].LCPDCPLLAPLNDSR.[V]	P12763	P12763 [145-159]	Hex(4)HexNAc(3)
[K].LCPDCPLLAPLNDSR.[V]	P12763	P12763 [145-159]	Hex(4)HexNAc(4)Fuc(4)
[K].LCPDCPLLAPLNDSR.[V]	P12763	P12763 [145-159]	Hex(5)HexNAc(4)
[K].LCPDCPLLAPLNDSR.[V]	P12763	P12763 [145-159]	Hex(5)HexNAc(4)
[K].LCPDCPLLAPLNDSR.[V]	P12763	P12763 [145-159]	Hex(5)HexNAc(4)

[K].LCPDCPLLAPLNDSR.[V]	P12763	P12763 [145-159]	Hex(5)HexNAc(4)
[K].LCPDCPLLAPLNDSR.[V]	P12763	P12763 [145-159]	Hex(6)HexNAc(5)NeuAc(1)
[K].LCPDCPLLAPLNDSR.[V]	P12763	P12763 [145-159]	Hex(5)HexNAc(4)Fuc(2)
[R].RPTGEVYDIEIDTLETTCHVLDPTPLANCSVR.[Q]	P12763	P12763 [72-103]	Hex(6)HexNAc(5)Fuc(1)
[R].RPTGEVYDIEIDTLETTCHVLDPTPLANCSVR.[Q]	P12763	P12763 [72-103]	Hex(5)HexNAc(4)Fuc(1)
[R].RPTGEVYDIEIDTLETTCHVLDPTPLANCSVR.[Q]	P12763	P12763 [72-103]	Hex(4)HexNAc(3)
[R].RPTGEVYDIEIDTLETTCHVLDPTPLANCSVR.[Q]	P12763	P12763 [72-103]	Hex(5)HexNAc(4)
[R].RPTGEVYDIEIDTLETTCHVLDPTPLANCSVR.[Q]	P12763	P12763 [72-103]	Hex(7)HexNAc(6)NeuAc(1)
[R].VVHAVEVALATFNAESNGSYLQLVEISR.[A]	P12763	P12763 [160-187]	Hex(6)HexNAc(5)NeuAc(1)
[R].VVHAVEVALATFNAESNGSYLQLVEISR.[A]	P12763	P12763 [160-187]	Hex(6)HexNAc(5)
[R].VVHAVEVALATFNAESNGSYLQLVEISR.[A]	P12763	P12763 [160-187]	Hex(6)HexNAc(5)NeuAc(1)
[R].VVHAVEVALATFNAESNGSYLQLVEISR.[A]	P12763	P12763 [160-187]	Hex(6)HexNAc(5)
[R].VVHAVEVALATFNAESNGSYLQLVEISR.[A]	P12763	P12763 [160-187]	Hex(6)HexNAc(5)Fuc(2)
[R].VVHAVEVALATFNAESNGSYLQLVEISR.[A]	P12763	P12763 [160-187]	Hex(6)HexNAc(5)
[R].VVHAVEVALATFNAESNGSYLQLVEISR.[A]	P12763	P12763 [160-187]	Hex(6)HexNAc(5)
[R].VVHAVEVALATFNAESNGSYLQLVEISR.[A]	P12763	P12763 [160-187]	Hex(6)HexNAc(5)NeuAc(1)
[R].VVHAVEVALATFNAESNGSYLQLVEISR.[A]	P12763	P12763 [160-187]	Hex(6)HexNAc(5)
[R].VVHAVEVALATFNAESNGSYLQLVEISR.[A]	P12763	P12763 [160-187]	Hex(5)HexNAc(4)

[R].VVHAVEVALATFNAESNGSYLQLVEISR.[A]	P12763	P12763 [160-187]	Hex(6)HexNAc(5)NeuAc(1)
[R].VVHAVEVALATFNAESNGSYLQLVEISR.[A]	P12763	P12763 [160-187]	Hex(6)HexNAc(5)
[R].VVHAVEVALATFNAESNGSYLQLVEISR.[A]	P12763	P12763 [160-187]	Hex(5)HexNAc(4)
[R].VVHAVEVALATFNAESNGSYLQLVEISR.[A]	P12763	P12763 [160-187]	Hex(6)HexNAc(5)
[R].VVHAVEVALATFNAESNGSYLQLVEISR.[A]	P12763	P12763 [160-187]	Hex(6)HexNAc(5)
[R].VVHAVEVALATFNAESNGSYLQLVEISR.[A]	P12763	P12763 [160-187]	Hex(6)HexNAc(5)
[R].VVHAVEVALATFNAESNGSYLQLVEISR.[A]	P12763	P12763 [160-187]	Hex(6)HexNAc(5)

Supplementary References

1. J. Jumper, R. Evans, A. Pritzel, T. Green, M. Figurnov, O. Ronneberger, K. Tunyasuvunakool, R. Bates, A. Žídek, A. Potapenko, A. Bridgland, C. Meyer, S. A. A. Kohl, A. J. Ballard, A. Cowie, B. Romera-Paredes, S. Nikolov, R. Jain, J. Adler, T. Back, S. Petersen, D. Reiman, E. Clancy, M. Zielinski, M. Steinegger, M. Pacholska, T. Berghammer, S. Bodenstein, D. Silver, O. Vinyals, A. W. Senior, K. Kavukcuoglu, P. Kohli and D. Hassabis, Highly accurate protein structure prediction with AlphaFold, *Nature*, 2021, **596**, 583-589.
2. T. Nishikaze, H. Tsumoto, S. Sekiya, S. Iwamoto, Y. Miura and K. Tanaka, Differentiation of Sialyl Linkage Isomers by One-Pot Sialic Acid Derivatization for Mass Spectrometry-Based Glycan Profiling, *Anal. Chem.*, 2017, **89**, 2353-2360.
3. G. W. T. M. J. Frisch, H. B. Schlegel, G. E. Scuseria,, J. R. C. M. A. Robb, G. Scalmani, V. Barone, B. Mennucci,, H. N. G. A. Petersson, M. Caricato, X. Li, H. P. Hratchian,, J. B. A. F. Izmaylov, G. Zheng, J. L. Sonnenberg, M. Hada,, K. T. M. Ehara, R. Fukuda, J. Hasegawa, M. Ishida, T. Nakajima,, O. K. Y. Honda, H. Nakai, T. Vreven, J. A. Montgomery, Jr.,, F. O. J. E. Peralta, M. Bearpark, J. J. Heyd, E. Brothers,, V. N. S. K. N. Kudin, T. Keith, R. Kobayashi, J. Normand,, A. R. K. Raghavachari, J. C. Burant, S. S. Iyengar, J. Tomasi,, N. R. M. Cossi, J. M. Millam, M. Klene, J. E. Knox, J. B. Cross,, C. A. V. Bakken, J. Jaramillo, R. Gomperts, R. E. Stratmann,, A. J. A. O. Yazyev, R. Cammi, C. Pomelli, J. W. Ochterski,, K. M. R. L. Martin, V. G. Zakrzewski, G. A. Voth,, J. J. D. P. Salvador, S. Dapprich, A. D. Daniels,, J. B. F. O. Farkas, J. V. Ortiz, J. Cioslowski, and a. D. J. Fox, Gaussian 09 Revision E.01, *Gaussian, Inc., Wallingford CT*, 2009.
4. A. D. Becke, A New Mixing Of Hartree-Fock And Local Density-Functional Theories, *J. Chem. Phys.*, 1993, **98**, 1372-1377.
5. W. L. Jorgensen, J. Chandrasekhar, J. D. Madura, R. W. Impey and M. L. Klein, Comparison of simple potential functions for simulating liquid water, *J. Chem. Phys.*, 1983, **79**, 926-935.
6. J. A. Maier, C. Martinez, K. Kasavajhala, L. Wickstrom, K. E. Hauser and C. Simmerling, ff14SB: Improving the Accuracy of Protein Side Chain and Backbone Parameters from ff99SB, *J. Chem. Theory Comput.*, 2015, **11**, 3696-3713.
7. K. B. D.A. Case, I.Y. Ben-Shalom, S.R. Brozell, D.S. Cerutti, T.E. Cheatham, III, V.W.D. Cruzeiro, T.A. Darden, R.E. Duke, G. Giambasu, M.K. Gilson, H. Gohlke, A.W. Goetz, R. Harris, S. Izadi, S.A. Izmailov, K. Kasavajhala, A. Kovalenko, R. Krasny, T. Kurtzman, T.S. Lee, S. LeGrand, P. Li, C. Lin, J. Liu, T. Luchko, R. Luo, V. Man, K.M. Merz, Y. Miao, O. Mikhailovskii, G. Monard, H. Nguyen, A. Onufriev, F.Pan, S. Pantano, R. Qi, D.R. Roe, A. Roitberg, C. Sagui, S. Schott-Verdugo, J. Shen, C.L. Simmerling, N.R.Skrynnikov, J. Smith, J. Swails, R.C. Walker, J. Wang, L. Wilson, R.M. Wolf, X. Wu, Y. Xiong, Y. Xue, D.M. York and P.A. Kollman, AMBER 2020, *University of California, San Francisco.*, 2020.
8. T. Darden, D. York and L. Pedersen, Particle mesh Ewald: An N·log(N) method for Ewald sums in large systems, *J. Chem. Phys.*, 1993, **98**, 10089-10092.

9. J.-P. Ryckaert, G. Ciccotti and H. J. C. Berendsen, Numerical integration of the cartesian equations of motion of a system with constraints: molecular dynamics of n-alkanes, *J. Comput. Phys.*, 1977, **23**, 327-341.
10. J.-W. Chu, B. L. Trout and B. R. Brooks, A super-linear minimization scheme for the nudged elastic band method, *J. Chem. Phys.*, 2003, **119**, 12708-12717.
11. B. P. Uberuaga, M. Anghel and A. F. Voter, Synchronization of trajectories in canonical molecular-dynamics simulations: Observation, explanation, and exploitation, *J. Chem. Phys.*, 2004, **120**, 6363-6374.
12. D. J. Sindhikara, S. Kim, A. F. Voter and A. E. Roitberg, Bad Seeds Sprout Perilous Dynamics: Stochastic Thermostat Induced Trajectory Synchronization in Biomolecules, *J. Chem. Theory Comput.*, 2009, **5**, 1624-1631.
13. Y. Zhang, S. E. Feller, B. R. Brooks and R. W. Pastor, Computer simulation of liquid/liquid interfaces. I. Theory and application to octane/water, *J. Chem. Phys.*, 1995, **103**, 10252-10266.
14. J. Li, G. Rossetti, J. Dreyer, S. Raugei, E. Ippoliti, B. Lüscher and P. Carloni, Molecular Simulation-Based Structural Prediction of Protein Complexes in Mass Spectrometry: The Human Insulin Dimer, *PLOS Comput. Biol.*, 2014, **10**, e1003838.
15. J. Li, W. Lyu, G. Rossetti, A. Konijnenberg, A. Natalello, E. Ippoliti, M. Orozco, F. Sobott, R. Grandori and P. Carloni, Proton Dynamics in Protein Mass Spectrometry, *J. Phys. Chem. Lett.*, 2017, **8**, 1105-1112.
16. L. Liu, X. Dong, Y. Liu, N. Österlund, A. Gräslund, P. Carloni and J. Li, Role of hydrophobic residues for the gaseous formation of helical motifs, *Chem. Commun. (Camb)*, 2019, **55**, 5147-5150.
17. A. Luzar and D. Chandler, Structure And Hydrogen-Bond Dynamics Of Water-Dimethyl Sulfoxide Mixtures by Computer-Simulations, *J. Chem. Phys.*, 1993, **98**, 8160-8173.
18. E. Guardia, J. Marti, L. Garcia-Tarres and D. Laria, A molecular dynamics simulation study of hydrogen bonding in aqueous ionic solutions, *J. Mol. Liq.*, 2005, **117**, 63-67.